

# Exact potentials in multivariate Langevin equations

Tiemo Pedergnana\* and Nicolas Noiray†  
*CAPS Laboratory, Department of Mechanical and Process Engineering,  
ETH Zürich, Sonneggstrasse 3, 8092 Zürich, Switzerland*

Systems governed by a multivariate Langevin equation featuring an exact potential exhibit straightforward dynamics but are often difficult to recognize because, after a general coordinate change, the gradient flow becomes obscured by the Jacobian matrix of the mapping. We show how to identify such systems by understanding their transformation properties arising from the chain rule, and we use this basic technique to derive exact potentials for broadly studied models of nonlinear deterministic and stochastic oscillations.

## I. INTRODUCTION

In systems featuring exact potentials, the evolution of a  $n$ -dimensional set of variables  $x = (x_1, \dots, x_n)^T: \mathbb{R} \rightarrow \mathbb{R}^n$  over time  $t \in \mathbb{R}$  is governed by the Langevin equation with potential (LP) [1, 2]

$$\dot{x} = -\nabla \mathcal{V}(x, t) + \Xi, \quad (1)$$

where  $\nabla_i = \partial/\partial x_i$ ,  $\mathcal{V}: \mathbb{R}^n \rightarrow \mathbb{R}$  is the potential,  $\mathcal{F}_i = -\nabla_i \mathcal{V}(x, t)$  is the  $i$ th component of the restoring force  $\mathcal{F}$  and the vector  $\Xi = (\xi_1, \dots, \xi_n)^T: \mathbb{R} \rightarrow \mathbb{R}^n$  contains uncorrelated white noise sources  $\xi_i$ ,  $i = 1, \dots, n$  of equal intensity  $\Gamma$ . The individual entries  $\xi_i$  of  $\Xi$  are assumed to be delta-correlated:  $\langle \xi_i \xi_{i,\tau} \rangle = \Gamma \delta(\tau)$ , where  $\langle \cdot \rangle$  is the expected value operator,  $\langle \cdot \rangle_{,\tau}$  denotes a positive time shift by  $\tau$  and  $\delta$  is the Dirac delta function [3].

Well known, low-dimensional examples of LPs are the Stuart–Landau oscillator [4–6], which represents the normal form of a supercritical Hopf bifurcation [7], and the deterministically and stochastically averaged noise-driven Van der Pol oscillator [3, 8–10]. Multivariate systems governed by potentials are also found in the classic Kuramoto model [11, 12], swarming oscillators [13], classical many-body time crystals [14], networks of coupled limit cycles [10, 15, 16] and in models of noise-driven, self-sustained modes of annular cavities [17–20].

In general, multivariate dynamical systems do not possess an exact potential. While the problem of finding meaningful quasi-potentials in systems that are *not* governed by an exact potential has been tackled in the past [21], there are also many relevant multivariate systems subject to random noise *with* exact potentials. If one exists, knowing the exact potential is a great benefit because it fully determines the stochastic dynamics in the steady state. The problem practitioners face is that it is often difficult to perceive the existence of a potential when the system is described with transformed variables. This issue is addressed in this work.

In particular, we are concerned with identifying the presence of an underlying exact potential in general

noise-driven systems taking the form

$$\dot{x} = \mathcal{F}(x, t) + \mathcal{B}(x)\Xi, \quad (2)$$

where  $\mathcal{F}$  is a vector- and  $\mathcal{B}$  a  $n$ -by- $n$  tensor field [1]. With the knowledge of  $\mathcal{F}$ , assuming a LP (1), one can easily deduce if an exact potential  $\mathcal{V}$  exists for  $x$  by checking the following necessary and sufficient conditions (see Ref. [2], pp. 133–134):

$$\nabla_i \mathcal{F}_j = \nabla_j \mathcal{F}_i \quad (3)$$

for all  $i$  and  $j \neq i$ . However, if this condition is not fulfilled, this does not preclude the existence of an exact potential governing the original variables that were transformed into  $x$  via a certain nonlinear mapping. We therefore argue that, instead of applying Eq. (3), Eq. (2) should be compared to a LP after a coordinate change defined by an arbitrary mapping  $x = f(y)$ . Assuming purely additive noise in the equations governing the underlying potential system which transforms objectively under local rotations and reflections, the resulting transformed Langevin equation with potential (TLP) reads, after redefining  $y \rightarrow x$ ,

$$\dot{x} = -g^{-1}(x)\nabla \tilde{\mathcal{V}}(x, t) + h^{-1}(x)\Xi, \quad (4)$$

where the Jacobian of  $f$ ,

$$J(x) = \nabla f(x), \quad (5)$$

was assumed to be nonsingular (invertible) with polar decomposition  $J = Qh$ ,  $Q = Q^{-T}$  is orthogonal,  $g = h^T h$  is the positive definite metric tensor and

$$\tilde{\mathcal{V}}(x, t) = \mathcal{V}(f(x), t) \quad (6)$$

is the transformed potential.

In this work, we derive necessary and sufficient conditions for the existence of an exact potential in a noise-driven system given by Eq. (2). After briefly recalling some of the special properties of potential systems driven by purely additive noise (PANs), we study their transformation rules under the mapping  $f$  from a continuum-mechanical perspective before applying our results to broadly studied examples of nonlinear oscillatory systems.

\* ptiemo@ethz.ch

† noiray@ethz.ch

## II. NOISE-DRIVEN POTENTIAL FLOWS

In this section, we list a few of the simplifications, compared to general dynamical systems, which offer themselves for PANs. We first analyze the stochastic case with  $\Gamma \neq 0$  using the Fokker-Planck equation (FPE), which describes the evolution of the joint probability density function  $P: \mathbb{R}^n \rightarrow \mathbb{R}$  of a random dynamic variable  $x$  over time [1, 2]. The FPE associated with the LP (1) reads

$$\frac{\partial P(x, t)}{\partial t} = \nabla \cdot [P(x, t) \nabla \mathcal{V}(x, t) + \frac{\Gamma}{2} \nabla P(x, t)]. \quad (7)$$

Without loss of generality, we make the substitution

$$P(x, t) = G(x, t) \exp\left(\frac{-2\mathcal{V}(x, t)}{\Gamma}\right), \quad (8)$$

which leads to an advection-diffusion equation for  $G$ :

$$\frac{\partial G(x, t)}{\partial t} + v(x, t) \cdot \nabla G(x, t) = \frac{\Gamma}{2} \nabla^2 G(x, t), \quad (9)$$

where  $v(x, t) = -\nabla \mathcal{V}(x, t)$  is the unsteady velocity field of the gradient flow. Equation (9) is analytically solvable in special cases [22–24]. Of special interest is the exact solution of Eq. (9) for a steady potential  $\partial \mathcal{V} / \partial t = 0$  given by  $G = \text{const.}$ , which corresponds to the stationary PDF  $P(x, t \rightarrow \infty) = P_\infty(x)$ :

$$P_\infty(x) = \mathcal{N} \exp\left(\frac{-2\mathcal{V}(x)}{\Gamma}\right), \quad (10)$$

where  $\mathcal{N} \in \mathbb{R}^+$  is a normalization constant. As shown below, the stationary PDF of the TLP (4) can be derived in analogous fashion:

$$\tilde{P}_\infty(x) = \mathcal{N} \exp\left(\frac{-2\tilde{\mathcal{V}}(x)}{\Gamma}\right). \quad (11)$$

In the deterministic limit  $\Gamma = 0$  and for time varying potential, the TLP (4) is reduced to the transformed gradient system

$$\dot{x} = -g^{-1}(x) \nabla \tilde{\mathcal{V}}(x, t). \quad (12)$$

Equation (12) states that trajectories  $x(t)$  are attracted to lower values of the potential  $\tilde{\mathcal{V}}$ , the attraction being equal to the potential gradient scaled with the inverse metric tensor  $g^{-1}$ . By definition and by the positive definiteness of  $g$ ,  $\tilde{\mathcal{V}}$  is a Lyapunov function of the variables  $x$  evolving under Eq. (12) and thus it determines the local and global stability of its trajectories [25].

## III. TRANSFORMATION RULES

### A. Gradient flow

We now derive the transformation rules for PANs given by Eq. (1), beginning with the gradient term. We use

the Einstein summation convention by which repeated indices in a product imply summation over these indices. In index form, the LP (1) with  $\Xi = 0$  reads

$$\dot{x}_k = -\frac{d\mathcal{V}(x, t)}{dx_k}, \quad (13)$$

for  $k = 1, \dots, n$ , where the partial  $x$ -derivatives in  $\nabla$  have been rewritten as total derivatives because  $\mathcal{V}$  depends only on the (spatially) independent variables  $x$  and  $t$ . Under the transformation  $x = f(y)$ , suppressing for brevity the dependence of  $f$  on  $y$  in the argument of  $\mathcal{V}$ , Eq. (13) becomes

$$\begin{aligned} \frac{df_k(y)}{dy_i} \frac{dy_i}{dt} &= -\frac{dy_j}{dx_k} \frac{d\mathcal{V}(f, t)}{dy_j} \\ &= -\frac{dy_j}{df_k(y)} \frac{d\mathcal{V}(f, t)}{dy_j}, \end{aligned} \quad (14)$$

which can be rewritten as

$$\frac{dy_i}{dt} = -\frac{dy_i}{df_k(y)} \frac{dy_j}{df_k(y)} \frac{d\mathcal{V}(f, t)}{dy_j}. \quad (15)$$

The formula for the squared length of an infinitesimal line element  $ds^2$  in general curvilinear coordinates  $y$  is

$$ds^2 = g_{ij} dy_i dy_j, \quad (16)$$

and the value of this quantity is independent of the coordinate system [26]. To relate  $ds^2$  to the original coordinates  $x$ , we consider the case where the mapping  $f$  is simply the identity:  $x = y$ . This gives  $g_{ij} = I_{ij}$ , where  $I$  is the identity matrix, so that

$$ds^2 = dx_k dx_k. \quad (17)$$

Multiplying both sides of Eq. (15) with  $g_{ij}$ , using Eq. (17) and noting that  $df_k = dx_k$ , we obtain

$$g_{ij} \frac{dy_i}{dt} = -\frac{d\mathcal{V}(f, t)}{dy_j}, \quad (18)$$

which can, by the symmetry of the metric tensor  $g$ , be written in vector form as follows:

$$\dot{y} = -g^{-1}(y) \nabla_y \tilde{\mathcal{V}}(y, t), \quad (19)$$

where  $(\nabla_y)_i = \partial / \partial y_i$  and the transformed potential was defined as  $\tilde{\mathcal{V}}(y, t) = \mathcal{V}(f(y), t)$ . As before, we interchanged partial and total derivatives in going from Eq. (18) to Eq. (19) because  $\tilde{\mathcal{V}}$  depends on  $y$  solely through  $f$ , and therefore the chain rule is the same for  $\partial \tilde{\mathcal{V}} / \partial y_j$  as for  $d\tilde{\mathcal{V}} / dy_j$ , i.e., the two terms coincide:

$$\frac{d\tilde{\mathcal{V}}(f, t)}{dy_j} = \frac{d\tilde{\mathcal{V}}(f, t)}{df} \frac{df}{dy_j} \quad (20)$$

$$= \frac{\partial \tilde{\mathcal{V}}(f, t)}{\partial f} \frac{\partial f}{\partial y_j}. \quad (21)$$

We then infer from Eq. (19) that under the mapping  $x = f(y)$ , the potential gradient transforms like

$$-\nabla \mathcal{V}(x, t) \rightarrow -g^{-1}(y) \nabla_y \tilde{\mathcal{V}}(y, t). \quad (22)$$

Redefining  $y \rightarrow x$  and  $\nabla_y \rightarrow \nabla$  in Eq. (19) yields Eq. (12).

## B. Noise term

Having studied the transformation properties of the deterministic gradient flow, we now turn to the noise term  $\Xi$  in Eq. (1). Knowing from Eq. (14) that under the mapping  $x = f(y)$ ,  $\dot{x}_k = J_{kj}\dot{y}_j$ , where  $J_{kj} = \partial f_k / \partial y_j$ , we can infer that  $\Xi$  transforms like

$$\Xi \rightarrow J^{-1}(y)\Xi(\tilde{\Xi}). \quad (23)$$

The problem one now faces is that it is not clear a priori how  $\Xi$  is related to the transformed noise vector  $\tilde{\Xi}$  i.e., the noise vector in  $y$ -coordinates. To resolve this issue, we assume that  $\tilde{\Xi}$  preserves the noise intensity and the local orientation of  $\Xi$  in the original coordinates. In other words, for  $x \rightarrow f(y)$ ,  $\Xi$  behaves like an objective vector field transformed by an orthogonal tensor field  $Q = Q^{-T}$  representing the local rotation or reflection associated with  $f$  [27]:

$$\Xi = Q(y)\tilde{\Xi}. \quad (24)$$

Note that  $Q$  can be directly obtained from the polar decomposition of the Jacobian of  $f$ :

$$J(y) = Q(y)h(y), \quad (25)$$

where  $h$  is a positive definite matrix (since  $J$  is, by assumption, invertible) of the same size as  $J$  and  $Q$ . Using Eqs. (24)-(25), the transformation formula (23) can be simplified as follows:

$$\Xi \rightarrow h^{-1}(y)\tilde{\Xi}. \quad (26)$$

Combining Eqs. (22) and (26) yields the TLP for systems with purely additive noise:

$$\dot{y} = -g^{-1}(y)\nabla_y \tilde{\mathcal{V}}(y, t) + h^{-1}(y)\tilde{\Xi}. \quad (27)$$

Redefining  $y \rightarrow x$ ,  $\nabla_y \rightarrow \nabla$  and  $\tilde{\Xi} \rightarrow \Xi$  reduces Eq. (27) to Eq. (4).

We stress that the assumptions made on the noise term in order to obtain Eq. (24) are not trivial, and that there may be situations where multiplicative noise terms appear that do not transform according to the same formula. Nevertheless, the special case described by Eq. (4) correctly identifies the exact potentials in the examples presented below.

## C. Fokker–Planck equation

The probability  $\mathcal{P}$  of the state  $x$  being inside the domain  $\mathcal{D}$  at time  $t$  is defined as

$$\mathcal{P} = \int_{\mathcal{D}} P(x, t) dV, \quad (28)$$

where  $dV = dx_1, \dots, dx_n$  is the volume element. In  $y$ -coordinates, using  $\det(J) = \det(h)$ , where  $\det$  is the determinant, Eq. (28) can be rewritten as

$$\mathcal{P} = \int_{\tilde{\mathcal{D}}} P(f(y), t) |\det(h(y))| d\tilde{V}, \quad (29)$$

where  $d\tilde{V} = dy_1, \dots, dy_n$  is the transformed volume element and  $\tilde{\mathcal{D}} = f^{-1}(\mathcal{D})$  is the transformed domain. We learn from Eq. (29) that the PDF  $P$  transforms like

$$P(x, t) \rightarrow |\det(h(y))| P(f(y), t) \quad (30)$$

under the mapping  $x = f(y)$ . Given a TLP (4), one can directly obtain  $\det(h)$  by computing the determinant of the matrix  $h^{-1}$  and using  $\det(h^{-1}) = \det(h)^{-1}$ . Typically, however, there is no interest in this geometric prefactor and the quantity of importance is the transformed PDF

$$\tilde{P}(y, t) = P(f(y), t). \quad (31)$$

Comparing Eq. (10) to Eq. (30), we observe that the steady-state solution  $P_\infty$  of the LP (1) with stationary potential transforms under  $f$  like

$$P_\infty(x) \rightarrow |\det(h(y))| \tilde{P}_\infty(y). \quad (32)$$

Knowledge of  $\tilde{\mathcal{V}}$  is sufficient to deduce the transformed stationary PDF

$$\tilde{P}_\infty(y) = \mathcal{N} \exp\left(\frac{-2\tilde{\mathcal{V}}(y)}{\Gamma}\right), \quad (33)$$

which, after redefining  $y \rightarrow x$ , coincides with Eq. (11).

## IV. POTENTIAL IDENTIFICATION

In the stochastic case, if  $\Xi$  is an additive noise vector with nonzero entries satisfying the assumptions made in the previous section and  $\mathcal{B}$  is nonsingular, identifying the exact potential  $\tilde{\mathcal{V}}$  of a general noise-driven system (2) is straightforward. By comparison with the TLP (4),  $h$  and  $g = h^T h$  are directly obtained from Eq. (2):

$$h(x) = \mathcal{B}^{-1}(x), \quad (34)$$

$$g(x) = \mathcal{B}^{-T}(x)\mathcal{B}^{-1}(x). \quad (35)$$

We recall that three-dimensional potential systems are uniquely defined by the vector identity

$$\text{curl grad}(\cdot) = 0, \quad (36)$$

i.e., the curl of a vector field is zero if and only if the vector field can be written as the gradient of a scalar function. Generalized to arbitrary dimensions, the equivalent identity reads

$$\text{skew}[\nabla^2(\cdot)] = 0, \quad (37)$$

where  $\text{skew}(\cdot)$  is the skew-symmetric part and  $\nabla^2(\cdot)$  is the Hessian matrix. By comparing Eqs. (2) and (4) and using  $h^T h = g$ , then, the following criteria are readily deduced:

- (I) A general noise-driven system described by Eq. (2) has an exact potential if and only if there exists a positive definite symmetric tensor field  $M$  such that

$$\text{skew}(\nabla[M(x)\mathcal{F}(x)]) = 0.$$

(II) For nonzero additive noise  $\Xi \neq 0$  satisfying the assumptions made in Sec. III B and nonsingular  $\mathcal{B}$ , a noise-driven system given by Eq. (2) has an exact potential if and only if

$$\text{skew}(\nabla[\mathcal{B}^{-T}(x)\mathcal{B}^{-1}(x)\mathcal{F}(x)]) = 0.$$

If either (I) or (II) are satisfied, the term in the square bracket is proportional to the potential gradient. If (I) is satisfied,  $M$  is proportional to the metric tensor  $g$ . Note that in the purely deterministic case  $\Xi = 0$ , (II) does not apply.

The general criterion (I) involves the solution of an underdetermined system of ordinary differential equations for a matrix  $M$  whose entries are constrained by its symmetry and positive definiteness, and is impractical for manual analysis. In the future, this criterion may be simplified or solved with computer algebra. In practice, low-dimensional gradient systems with  $\Xi = 0$  are identified by inspection of Eq. (2) under consideration of the general form of a TLP (4). Specific examples are discussed below.

## V. EXAMPLES

We now demonstrate our method on some of the examples mentioned in Sec. I. The goal of this section is to create a reference base of commented solutions to potential identification problems of varying complexity. All equations are presented in the same form in which they appear in the references, up to minor changes in notation.

### A. Averaged Van der Pol oscillator

The weakly nonlinear dynamics of a harmonically forced, noise-driven Van der Pol oscillator synchronized with the forcing frequency  $\omega$  can be derived using deterministic and stochastic averaging. The resulting equations are given, up to a typographical error [28], by Eqs. (7.58) and (7.59) of Ref. [10]:

$$\dot{A} = \frac{A}{2}(\lambda - \frac{A^2}{4}) - \frac{F}{2\omega} \sin \varphi + \frac{\Gamma}{4A\omega^2} + \eta_1, \quad (38)$$

$$\dot{\varphi} = \Delta - \frac{F}{2\omega A} \cos \varphi + \frac{\eta_2}{A}, \quad (39)$$

where  $\Delta = (\omega_0^2 - \omega^2)/2\omega \approx \omega_0 - \omega$  is the detuning between the eigen- ( $\omega_0$ ) and the forcing ( $\omega$ ) frequency,  $2\sqrt{\lambda}$  is the limit cycle amplitude,  $F$  is the forcing amplitude,  $\Xi = (\eta_1, \eta_2)^T$  and  $\eta_{1,2}$  are uncorrelated white noise sources of equal intensity  $\Gamma/2\omega^2$ .

Defining the new variables  $x = (A, \Phi)^T$ , where  $\Phi = \varphi - \Delta t$ , by criterion (II), Eqs. (38)-(39) have the form of a TLP with  $g(x) = \text{diag}(1, A^2)$ ,  $h(x) = \text{diag}(1, A)$  and

$$\tilde{\mathcal{V}}(x, t) = -\frac{A^2\lambda}{4} + \frac{A^4}{32} + \frac{AF}{2\omega} \sin(\Phi + \Delta t) - \frac{\Gamma}{4\omega^2} \ln A.$$

## B. Generalized Kuramoto model

In Ref. [13], a set of swarming oscillators (“swarmalators”) is governed by a generalized Kuramoto model:

$$\dot{y}_i = \nu_i + \frac{\mathcal{J}}{N} \sum_j^N \sin(y_j - y_i) \cos(\theta_j - \theta_i), \quad (40)$$

$$\dot{\theta}_i = \omega_i + \frac{\mathcal{K}}{N} \sum_j^N \cos(y_j - y_i) \sin(\theta_j - \theta_i), \quad (41)$$

where  $i = 1, \dots, N$ ,  $n = 2N$  is the system dimension, the parameters  $\mathcal{J}, \mathcal{K} \in \mathbb{R}$  are coupling constants and  $\nu_i, \omega_i \in \mathbb{R}$  are the eigenfrequencies of the dynamic variables  $y_i$  and  $\theta_i$ . To observe the exact potential, we define the new variables  $x = (Y_1, \dots, Y_N, \Theta_1, \dots, \Theta_N)^T$ , where  $Y_i = y_i/\mathcal{J}$  and  $\Theta_i = \theta_i/\mathcal{K}$ . The resulting system is a transformed gradient system with  $g = \text{diag}(\mathcal{J}, \dots, \mathcal{J}, \mathcal{K}, \dots, \mathcal{K}) \in \mathbb{R}^n$  and

$$\begin{aligned} \tilde{\mathcal{V}}(x) = -\sum_k^N \left[ \frac{1}{2N} \sum_j^N \cos \mathcal{J}(Y_j - Y_k) \cos \mathcal{K}(\Theta_j - \Theta_k) \right. \\ \left. + \nu_k Y_k + \omega_k \Theta_k \right]. \end{aligned} \quad (42)$$

## C. Classical time crystal

The dynamics of a classical many-body time crystal are studied in [14], leading to a system of even dimension  $n = 2N$  with linear dynamics

$$\begin{aligned} \dot{z} = & \begin{pmatrix} a & b & b & \dots \\ b & a & b & \\ b & b & a & \\ \vdots & & & \ddots \end{pmatrix} z \\ = & Az. \end{aligned} \quad (43)$$

The sub-matrices  $a, b \in \mathbb{R}^{2 \times 2}$  are

$$\begin{aligned} a = & \begin{pmatrix} -\frac{\gamma}{2} & -\frac{\lambda\omega_0^2 + 2(\omega_0^2 - \omega^2)}{4\omega} \\ -\frac{\lambda\omega_0^2 + 2(\omega_0^2 - \omega^2)}{4\omega} & -\frac{\gamma}{2} \end{pmatrix}, \\ b = & \begin{pmatrix} 0 & \frac{\beta^2}{2\omega N} \\ -\frac{\beta^2}{2\omega N} & 0 \end{pmatrix}, \end{aligned}$$

where  $\gamma$  is the dissipation,  $\lambda$  is the parametric driving strength,  $\omega_0$  is the eigen- and  $2\omega$  is the parametric driving frequency. For simplicity, we consider a 4-by-4 block of Eq. (43) with variables  $z = (z_1, z_2, z_3, z_4)^T$ ,  $N = 2$  and

$$A = \begin{pmatrix} a & b \\ b & a \end{pmatrix}. \quad (44)$$

The non-symmetric matrices populating the anti-diagonal of  $A$  indicate the presence of reactive coupling which obstructs the direct identification of the potential. To circumvent this issue, we first make a transformation  $z = f(y)$  to amplitude-phase coordinates  $y = (A_1, A_2, \varphi_1, \varphi_2)^T$ :

$$z = \begin{pmatrix} A_1 \cos \varphi_1 \\ A_2 \cos \varphi_2 \\ A_2 \sin \varphi_2 \\ A_1 \sin \varphi_1 \end{pmatrix}. \quad (45)$$

The dynamics of the  $y$ -coordinates equivalent to Eq. (43) are

$$\dot{y} = \begin{pmatrix} -\frac{\gamma A_1}{2} - \frac{\lambda \omega_0^2 + 2(\omega_0^2 - \omega^2)}{4\omega} A_2 \cos(\varphi_1 - \varphi_2) \\ -\frac{\gamma A_2}{2} - \frac{\lambda \omega_0^2 + 2(\omega_0^2 - \omega^2)}{4\omega} A_1 \cos(\varphi_1 - \varphi_2) \\ -\frac{\beta^2}{4\omega} + \frac{\lambda \omega_0^2 + 2(\omega_0^2 - \omega^2)}{4\omega} \frac{A_2}{A_1} \sin(\varphi_1 - \varphi_2) \\ \frac{\beta^2}{4\omega} - \frac{\lambda \omega_0^2 + 2(\omega_0^2 - \omega^2)}{4\omega} \frac{A_1}{A_2} \sin(\varphi_1 - \varphi_2) \end{pmatrix},$$

which, defining the new variables  $x = (A_1, A_2, \Phi_1, \Phi_2)^T$  with  $\Phi_{1,2} = \varphi_{1,2} \pm \beta^2 t / 4\omega$ , corresponds to a transformed gradient system with  $g(x) = \text{diag}(1, 1, A_1^2, A_2^2)$  and

$$\tilde{\mathcal{V}}(x, t) = \frac{\gamma(A_1^2 + A_2^2)}{4} + \frac{\lambda \omega_0^2 + 2(\omega_0^2 - \omega^2)}{4\omega} A_1 A_2 \cos(\Phi_1 - \Phi_2 - \frac{\beta^2 t}{2\omega}). \quad (46)$$

#### D. Coupled limit cycles

The weakly nonlinear amplitude-phase dynamics of two linearly coupled Van der Pol oscillators, derived using deterministic averaging, are given by Eq. (4.11) of Ref [10]:

$$\dot{A}_1 = \frac{\lambda_1}{2} A_1 - \frac{1}{8} A_1^3 + \frac{C}{2} (A_2 \cos \phi - A_1), \quad (47)$$

$$\dot{A}_2 = \frac{\lambda_2}{2} A_2 - \frac{1}{8} A_2^3 + \frac{C}{2} (A_1 \cos \phi - A_2), \quad (48)$$

$$\dot{\phi} = \Delta - \frac{C}{2} \sin \phi \left( \frac{A_2}{A_1} + \frac{A_1}{A_2} \right), \quad (49)$$

where  $C$  is the coupling,  $\phi = \varphi_2 - \varphi_1$  is the phase difference and  $\Delta = (\omega_2^2 - \omega_1^2)/2\omega \approx \omega_2 - \omega_1$  is the detuning between the eigenfrequencies  $\omega_{1,2}$  and  $\omega$  is the frequency of the synchronized coupled oscillators  $\omega \approx \omega_{1,2}$ . If we define  $x = (A_1, A_2, \Phi)^T$ ,  $\Phi = \phi - \Delta t$ , then Eqs. (47)-(49) are equivalent a transformed gradient system with  $g^{-1}(x) = \text{diag}(1, 1, A_1^{-2} + A_2^{-2})$  and

$$\tilde{\mathcal{V}}(x, t) = -\frac{\lambda_1 A_1^2 + \lambda_2 A_2^2}{4} + \frac{A_1^4 + A_2^4}{32} + \frac{C}{4} [A_1^2 + A_2^2 - 2A_1 A_2 \cos(\Phi + \Delta t)]. \quad (50)$$

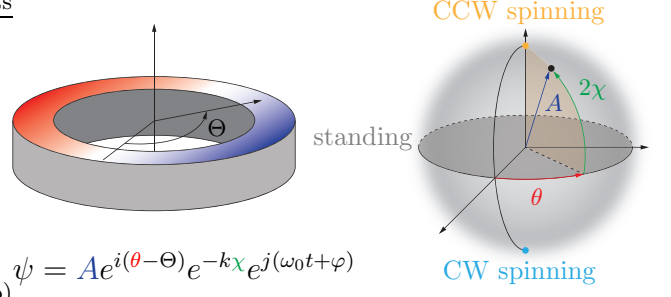


Figure 1. Illustration of the examples presented in Secs. VE and VF. In Refs. [18, 20, 29], a self-oscillating mode  $\psi$  in an annular cavity is projected onto four variables  $x = (A, \theta, \chi, \varphi)^T$  using the basic quaternions  $(i, j, k)$  (left inset). By this geometric analogy, different states such as pure spinning and standing waves are represented as different points on the Bloch sphere (right inset). The same coordinate system is used to represent the PDF isosurfaces in Fig. 2.

It is an open question whether the above results can simplify the stability analysis of Eqs. (47)-(49) (see Ref. [15] and Ref. [10], pp. 83–84).

#### E. Nonlinear coupling

In [17], the following set of nonlinearly coupled amplitude and phase equations are obtained by averaging the equation describing the projection of turbulence-driven thermoacoustic dynamics onto two orthogonal modes in an annular cavity (see Fig. 1, left inset for a sketch):

$$\begin{aligned} \dot{A} &= \nu A - \frac{3\kappa}{32} (3A^2 + [2 + \cos(2\phi)]B^2) A \\ &\quad + \frac{\Gamma}{4\omega_0^2 A} + \zeta_a, \end{aligned} \quad (51)$$

$$\begin{aligned} \dot{B} &= \nu B - \frac{3\kappa}{32} (3B^2 + [2 + \cos(2\phi)]A^2) B \\ &\quad + \frac{\Gamma}{4\omega_0^2 B} + \zeta_b, \end{aligned} \quad (52)$$

$$\dot{\phi} = \frac{3\kappa(A^2 + B^2)}{32} \sin(2\phi) + \left( \frac{1}{A} + \frac{1}{B} \right) \zeta_\phi, \quad (53)$$

where  $A$  and  $B$  are the amplitudes,  $\phi = \varphi_a - \varphi_b$  is the phase difference,  $\omega_0$  is the eigenfrequency,  $\nu$  is the growth rate,  $\kappa$  is the nonlinearity constant,  $\Xi = (\zeta_a, \zeta_b, \zeta_\phi)^T$  and  $\zeta_a, \zeta_b, \zeta_\phi$  are white noise sources of equal intensity  $\Gamma/2\omega_0^2$ . Equation (53) can be rewritten as two separate equations for the phases  $\varphi_a$  and  $\varphi_b$ :

$$\dot{\varphi}_a = \frac{3\kappa B^2}{32} \sin 2(\varphi_a - \varphi_b) + \frac{\zeta_a}{A}, \quad (54)$$

$$\dot{\varphi}_b = -\frac{3\kappa A^2}{32} \sin 2(\varphi_a - \varphi_b) + \frac{\zeta_b}{B}, \quad (55)$$

where  $\zeta_{a,b}$  are white noise sources of intensity  $\Gamma/2\omega_0^2$ . Starting from Eqs. (54)-(55), Eq. (53) can be derived by

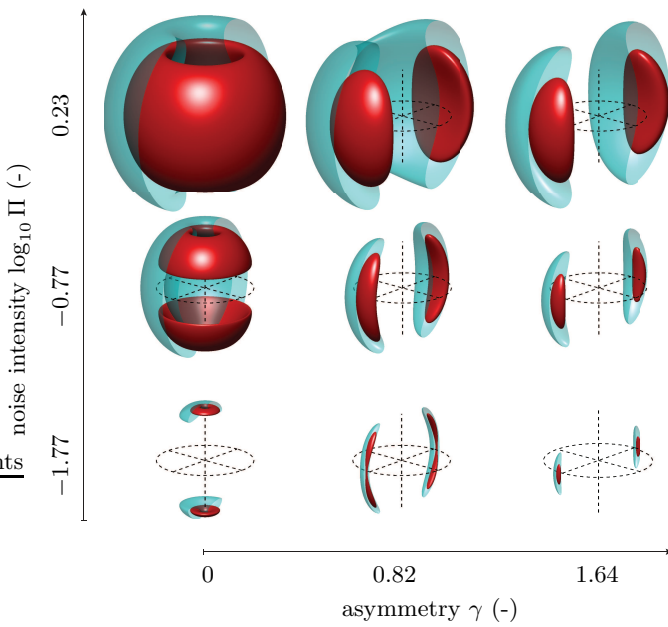


Figure 2. Illustration of the results derived in Sec. V F. Shown are isosurfaces of the transformed stationary PDF  $\tilde{P}_\infty$  given by Eqs. (11) and (63) corresponding to one (red) and three (cyan) fourths of its maximum value, as a function of the nondimensionalized noise intensisity  $\Pi$  and asymmetry  $\gamma$  (semi-log scale, definitions in Eqs. (64)-(65)). The spherical coordinate system used to represent the PDF is defined in Figure 1. The length of the dashed vertical line and the dashed circle's radius are both equal to  $8\sqrt{\nu/15\kappa}$ . The spatial structure of the analytical Fokker-Planck solution shown in this figure is in excellent agreement with the numerical simulations presented in Fig. 11 of Ref. [20].

taking the difference between the former two equations and setting  $\xi_a = -\xi_b = \zeta_\phi$ .

According to criterion (II), Eqs. (51), (52), (54) and (55) correspond to a TLP with  $x = (A, B, \varphi_a, \varphi_b)^T$ ,  $\Xi = (\zeta_a, \zeta_b, \xi_a, \xi_b)^T$ ,  $g(x) = \text{diag}(1, 1, A^2, B^2)$ ,  $h(x) = \text{diag}(1, 1, A, B)$  and

$$\begin{aligned} \tilde{\mathcal{V}}(x) = & -\frac{\nu(A^2 + B^2)}{2} + \frac{3\kappa}{128}(3(A^4 + B^4) \\ & + 2A^2B^2[2 + \cos 2(\varphi_a - \varphi_b)]) \\ & - \frac{\Gamma}{4\omega_0^2} \ln(AB). \end{aligned} \quad (56)$$

### F. Quaternion flow

In the study of self-oscillating thermoacoustic modes in annular cavities, an alternative projection to the one used in [17] and based on quaternions offers a convenient description of the nature of the modal dynamics, where one of the state variables indicates whether spinning or standing waves govern the dynamics at a given time instant [18–20, 29]. Indeed, by projecting the acoustic field

$\psi(\Theta, t)$  depending on the azimuthal angle  $\Theta$  onto the four alternative state variables  $x = (A, \chi, \theta, \varphi)^T$  using the basic quaternions  $(i, j, k)$ , as proposed first in [29] based on the quaternion Fourier transform for bivariate signals defined in [30], the instantaneous state can be mapped to different points on the Bloch sphere. In this representation, counter-clockwise (CCW) and clockwise (CW) spinning waves correspond to the north ( $2\chi = \pi/2$ ) and south ( $2\chi = -\pi/2$ ) poles, while the equatorial plane ( $\chi = 0$ ) describes pure standing waves (Fig. 1). In general, the system state is a mixture between a standing and a spinning wave. The variable  $\theta$  describes the orientation of the nodal line of  $\psi$  (line connecting the white regions in Fig. 1, left inset). In Ref. [18], the following dynamics for  $x$  are derived by deterministic and stochastic averaging of the projected acoustic wave equation:

$$\dot{x} = \mathcal{F}(x) + \mathcal{B}(x)\Xi. \quad (57)$$

The entries of the deterministic term  $\mathcal{F}$  in Eq. (57) are

$$\begin{aligned} \mathcal{F}_1 = & \left( \nu + \frac{c}{4} \cos(2\theta) \cos(2\chi) \right) A \\ & - \frac{3\kappa}{64} [5 + \cos(4\chi)] A^3 + \frac{3\Gamma}{4\omega_0^2 A}, \end{aligned} \quad (58)$$

$$\begin{aligned} \mathcal{F}_2 = & \frac{3\kappa}{64} A^2 \sin(4\chi) - \frac{c}{4} \cos(2\theta) \sin(2\chi) \\ & - \frac{\Gamma \tan(2\chi)}{2\omega_0^2 A^2}, \end{aligned} \quad (59)$$

$$\mathcal{F}_3 = -\frac{c \sin(2\theta)}{4 \cos(2\chi)}, \quad (60)$$

$$\mathcal{F}_4 = \frac{c}{4} \sin(2\theta) \tan(2\chi), \quad (61)$$

where  $\nu$  is the growth rate,  $\kappa$  is the nonlinearity constant,  $\omega_0$  is the eigenfrequency and  $c$  is the asymmetry. The entries of the noise vector  $\Xi = (\zeta_A, \zeta_\chi, \zeta_\theta, \zeta_\varphi)^T$  each have equal intensity  $\Gamma/2\omega_0^2$  and the matrix  $\mathcal{B}$  describing the stochastic coupling is given in the reference as

$$\mathcal{B} = \begin{pmatrix} 1 & 0 & 0 & 0 \\ 0 & A^{-1} & 0 & 0 \\ 0 & 0 & \frac{1}{A \cos 2\chi} & 0 \\ 0 & 0 & -\frac{\tan 2\chi}{A} & A^{-1} \end{pmatrix}. \quad (62)$$

By criterion (II), Eqs. (57)–(62), which coincide with those given in Ref. [19] for  $c = 0$  and rescaled noise intensity  $\Gamma/2\omega_0^2 \rightarrow \Gamma/2$ , describe a TLP with

$$g^{-1}(x) = \begin{pmatrix} 1 & 0 & 0 & 0 \\ 0 & A^{-2} & 0 & 0 \\ 0 & 0 & \frac{1}{A^2 \cos(2\chi)^2} & -\frac{\tan 2\chi}{A^2 \cos 2\chi} \\ 0 & 0 & -\frac{\tan 2\chi}{A^2 \cos 2\chi} & A^{-2} + \frac{\tan(2\chi)^2}{A^2} \end{pmatrix},$$

$$h^{-1}(x) = \mathcal{B}(x),$$

and the transformed potential

$$\begin{aligned}\tilde{\mathcal{V}}(x) = & -\left(\nu + \frac{c}{4} \cos(2\theta) \cos(2\chi)\right) \frac{A^2}{2} \\ & + \frac{3\kappa}{256} [5 + \cos(4\chi)] A^4 \\ & - \frac{3\Gamma}{4\omega_0^2} \ln(A) - \frac{\Gamma}{4\omega_0^2} \ln(\cos(2\chi)).\end{aligned}\quad (63)$$

In Fig. 2, we plot the transformed stationary PDF  $\tilde{P}_\infty(x)$  given by Eqs. (11) and (63) in the quasi-spherical coordinate system  $(A, 2\chi, \theta)$  on a semi-log scale for different values of the nondimensionalized noise intensity  $\Pi$  and asymmetry  $\gamma$ :

$$\Pi = \frac{27\kappa\Gamma}{256\nu^2\omega_0^2}, \quad (64)$$

$$\gamma = \frac{c}{2\nu}. \quad (65)$$

As  $\gamma$  is increased from zero, a preferred direction in  $\theta$  emerges in the steady state, demonstrating the explicitly broken symmetry of the system for  $\gamma \neq 0$ . The spatial structure of the analytical PDF  $\tilde{P}_\infty$  shown in Fig. 2 is

in excellent agreement with numerical simulations of the Fokker–Planck equation presented in Fig. 11 of Ref. [20].

## VI. CONCLUSIONS

In this study, we derived necessary and sufficient criteria for the existence of an exact potential in a general noise-driven system. We demonstrated on several broadly studied models of deterministic and stochastic oscillations that a basic understanding of the chain rule for transformed potential systems driven by additive noise can lead to new analytical descriptions of their nonlinear dynamics. The question arises *why* exact potentials appear to be ubiquitous in time-averaged systems; this is left for future research to answer.

## ACKNOWLEDGEMENTS

This project is funded by the Swiss National Science Foundation under Grant agreement 184617.

---

[1] C. W. Gardiner *et al.*, *Handbook of stochastic methods*, Vol. 4 (Springer Berlin, 1985).

[2] H. Risken, *The Fokker-Planck Equation* (Springer, 1996) pp. 63–95.

[3] R. Stratonovich, *Topics in the Theory of Random Noise Vol. I: General Theory of Random Processes Nonlinear Transformations of Signals and Noise* (Gordon & Breach, 1963).

[4] J. Stuart, *J. Fluid Mech.* **4** (1958).

[5] L. D. Landau and E. M. Lifshitz, *Fluid mechanics*, Vol. 11 (Pergamon Press Oxford, UK, 1959).

[6] M. Lax, *Phys. Rev.* **160**, 290 (1967).

[7] V. I. Arnold, *Geometrical methods in the theory of ordinary differential equations*, Vol. 250 (Springer Science & Business Media, 2012).

[8] B. Van der Pol, *London Edinburgh Philos. Mag. J. Sci.* **2**, 978 (1926).

[9] J. A. Sanders, F. Verhulst, and J. Murdock, *Averaging methods in nonlinear dynamical systems*, Vol. 59 (Springer, 2007).

[10] A. Balanov, N. Janson, D. Postnov, and O. Sosnovtseva, *From simple to complex* (Springer, 2009).

[11] Y. Kuramoto, in *Chemical oscillations, waves, and turbulence* (Springer, 1984) pp. 111–140.

[12] S. Strogatz, *Physica D* **143**, 1 (2000).

[13] K. O’Keeffe, S. Ceron, and K. Petersen, *Phys. Rev. E* **105** (2022).

[14] T. L. Heugel, M. Oscity, A. Eichler, O. Zilberberg, and R. Chitra, *Phys. Rev. Lett.* **123** (2019).

[15] D. Aronson, G. Ermentrout, and N. Kopell, *Physica D* **41** (1990).

[16] T. Pedergnana and N. Noiray, *Nonlinear Dyn.* **108** (2022).

[17] N. Noiray and B. Schuermans, *Proc. R. Soc. A* **469** (2013).

[18] A. Faure-Beaulieu and N. Noiray, *Phys. Rev. Fluids* **5** (2020).

[19] G. Ghirardo and F. Gant, *J. Sound Vib.* **490** (2021).

[20] T. Indlekofer, A. Faure-Beaulieu, J. R. Dawson, and N. Noiray, *J. Fluid Mech.* **944**, A15 (2022).

[21] J. Zhou, D. Aliyu, E. Aurell, and S. Huang, *J. R. Soc. Interface* **9**, 3539 (2012).

[22] J. Philip, *Water Resour. Res.* **30** (1994).

[23] C. Zoppou and J. Knight, *J. Hydraul. Eng.* **123** (1997).

[24] C. Zoppou and J. Knight, *Appl. Math. Model.* **23** (1999).

[25] A. Lyapunov, *Int. J. Control* **55**, 531 (1992).

[26] W. Kühnel, *Differential geometry*, Vol. 77 (American Mathematical Society, 2015).

[27] C. Truesdell and W. Noll, in *The non-linear field theories of mechanics* (Springer, 2004) pp. 1–579.

[28] The  $A^2$  in the bracket is missing in Eq. (7.58) of Ref. [10].

[29] G. Ghirardo and M. Bothien, *Phys. Rev. Fluids* **3** (2018).

[30] J. Flamant, N. Le Bihan, and P. Chainais, *Appl. Comput. Harmon. Anal.* **46**, 351 (2017).